Available online at www.sciencedirect.com
ScienceDirect
Trans. Nonferrous Met. Soc. China 21(2011) 1498−1505
Transactions of Nonferrous Metals Society of China
www.tnmsc.cn

Effect of ageing time on corrosion behavior of Mg-10Gd-4.8Y-0.6Zr extruded-alloy

LI Hui-zhong[1, 2, 3], LIU Hong-ting[1], GUO Fei-fei[1], WANG Hai-jun[1], LIANG Xiao-peng[1, 2], LIU Chu-ming[1]

1. School of Materials Science and Engineering, Central South University, Changsha 410083, China;
2. State Key Laboratory of Powder Metallurgy, Central South University, Changsha 410083, China;
3. Key Laboratory of Nonferrous Metal Materials Science and Engineering of Ministry of Education, Central South University, Changsha 410083, China

Received 17 March 2011; accepted 19 May 2011

Abstract: The corrosion behaviors of Mg-10Gd-4.8Y-0.6Zr extruded-alloys with various ageing time were investigated by immersion test and electrochemical measurements. The results show that the corrosion rate of the experimental alloy decreases with the increase of ageing time from 0 to 108 h. The corrosion resistance of the experimental alloy was found to increase with the increase of the size of the precipitate phases. The open circuit potential of the experimental alloy increases with the increase of the ageing time. The potentiodynamic polarization curves show that the cathodic over-potential increases with the increase of ageing time, leading to a decrease in the current density of anodic current plateau with the increase of ageing time.
Key words: Mg-10Gd-4.8Y-0.6Zr alloy; corrosion behavior; ageing time

1 Introduction

Magnesium alloys containing rare earth (RE) elements are becoming more attractive as light structural materials for spacecraft and automotive components because of their low density, high strength and good heat resistance. Recently, many researchers suggested that Mg-Gd-Y system alloys have higher strength at both room and elevated temperatures and better creep resistance than other Mg-RE alloys, such as WE54, WE43 and QE22 [1−6].

Many studies have been done to improve mechanical properties of Mg-Gd-Y-Zr alloys. HE et al [4] reported that solid solution strengthening, grain boundary strengthening and precipitation strengthening contributed to the strength of Mg-Gd-Y-Zr alloys. But there were relatively few investigations on the corrosion behavior of these alloys. Therefore, it is essential to study the corrosion of Mg-Gd-Y-Zr alloys under the environmental conditions. As we all know, Mg-Gd-Y-Zr alloys have always been used at high temperature circumstances of 200−300 °C, and these alloys have obvious age hardening at this temperature. KAMADO et al [7] studied the ageing behavior and found the precipitation sequence of the alloy as S.S.S.S.→β''($D0_{19}$)→β'(cbco)→β(bcc). HONMA et al [8] found that the precipitation sequence was S.S.S.S.→β''($D0_{19}$)→β'(cbco)→β_1(fcc)→β(bcc), which is similar to that of WE54 alloy. There are different phases of different ageing states in Mg-Gd-Y-Zr alloys. Therefore, it is necessary to investigate the corrosion behavior of Mg-10Gd-4.8Y-0.6Zr alloy during ageing treatment.

In the present study, the corrosion behavior of Mg-10Gd-4.8Y-0.6Zr alloy in different ageing states was investigated by using immersion test and electrochemical measurements. The effect of ageing treatment on corrosion behavior of the alloy was discussed.

2 Experimental

2.1 Sample preparation

Mg-10Gd-4.8Y-0.6Zr (mass fraction, %) alloy in cast condition was solution treated at 520 °C for 16 h, quenched into water, and then hot-extruded into rods with a diameter of 17.2 mm. The extrusion ratio was 11 and the ingot was heated to 400 °C before the extrusion process.

Foundation item: Project (51074186) supported by the National Natural Science Foundation of China
Corresponding author: LI Hui-zhong; Tel: +86-731-88830377; Fax: +86-731-88830257; E-mail: hzli606@gmail.com
DOI: 10.1016/S1003-6326(11)60887-X

Specimens cut from the extruded rods were aged at 200 °C for 0, 1, 8, 20 and 108 h for corrosion investigation. The microstructures of the aged alloy were observed with transmission electron microscope (TEM). Vicker hardness (HV) testing was taken using load of 4.9 N and holding time of 15 s. The specimens for immersion test were cut into plates of 5 mm in thickness and 30 mm in diameter on the wire cutting machine. A hole of 2.8 mm in diameter was drilled near one edge of each immersion specimen to suspend it using nylon thread in the test solution.

2.2 Immersion test

For the immersion tests, three replicated specimens were used under each condition of ageing treatment. The specimens were weighed for the original mass. Corrosion tests included 3 d of continuous immersion of specimens in 3.5% NaCl solution, exposed to laboratory conditions at a temperature of (25±2) °C. After the corrosion tests, the corroded specimens were photographed and then immersed into a 200 g/L chromate acid solution with 10 g/L silver nitrate at room temperature for 8 min to remove the corrosion products. Afterwards the specimens were quickly washed with distilled water, dried using a hair dryer and weighed for mass loss.

2.3 Electrochemical measurement

The electrochemical measurement was carried out in a 3.5% NaCl solution at room temperature. Variations of the open circuit potentials (φ_{OCP}), polarization curves and electrochemical impedance spectroscopy (EIS) were recorded by an IM6eX electrochemical analysis instrument. A saturated calomel electrode (SCE) and a platinum foil were used as reference electrode and counter electrode, respectively. For these electrochemical experiments, three replicated specimens of 10 mm×10 mm were cut from the aged alloy. The φ_{OCP} was recorded between the working electrode and reference electrode without current. φ_{OCP} measurement was performed directly for 1 200 s in 3.5% NaCl solution prior to polarization experiment and EIS to ensure the stability of the corrosion potential. The polarization test was made at a scan rate of 0.3 mV/s from −250 mV to 500 mV with respect to φ_{OCP}. EIS experiment was carried out in the frequency range from 100 kHz to 100 mHz.

3 Results and discussion

3.1 Ageing hardening behavior

Figure 1 shows the age-hardening curve of the extruded Mg-10Gd-4.8Y-0.6Zr alloy during ageing at 200 °C. At the beginning of ageing, the hardness increases rapidly with the ageing time until a peak value of hardness (HV 137) reaching at about 20 h. There is a plateau of peak-aging region from 20 h to 72 h. The hardness of alloy keeps a high level of about HV 135 at this plateau and then further ageing leads to a slow decrease in the hardness. It seems to be noticeable that the Mg-10Gd-4.8Y-0.6Zr alloy has a strong ageing strengthening effect. Many researchers [1, 3, 7] proved that ageing strengthening effect of Mg-Gd-Y-Zr alloys was induced due to different phases precipitated during the ageing process. KAMADO et al [7] found that the precipitation sequence of Mg-Gd-Y-Zr alloy was S.S.S.S.→$\beta''(D0_{19})$→β'(cbco)→β(bcc). The main purpose of this subject is to investigate the corrosion behavior of Mg-10Gd-4.8Y-0.6Zr alloy in different ageing stages. Thus ageing time of 0, 1, 8, 20 and 108 h was selected for corrosion investigation, which corresponded to non-aged, under-aged, half-peak, peak and over-aged conditions, respectively.

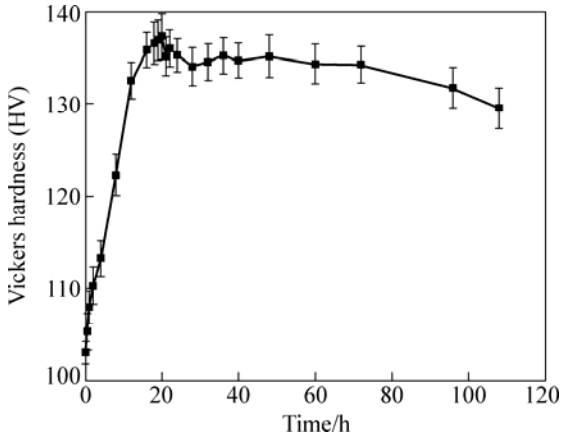

Fig. 1 Age-hardening curve of extruded Mg-10Gd-4.8Y- 0.6Zr alloy at 200 °C

3.2 Precipitate microstructures

In order to investigate the variety of precipitated phases during ageing treatment, ageing time of 8, 20 and 108 h was selected to observe the precipitate microstructures by transmission electron microscopy (TEM). Figure 2 shows TEM bright field images of the selected samples, with the corresponding selected area electron diffraction (SAED) patterns.

The bright field image of the sample aged for 8 h (Fig. 2(a)) shows an amount of fine precipitates, which consist of the metastable β'' and β' precipitate phases. Despite the fact that the sample aged for half-peak (8 h) shows no clear contrasts (Fig. 2(a)), the corresponding SAED pattern clearly reveals the presence of a hexagonal $D0_{19}$ structure phase. The orientation relationships between this phase and the α-Mg matrix are $(2\bar{1}\bar{1}0)_{\beta''}//(2\bar{1}\bar{1}0)_{\alpha}$. HONMA et al [8] suggested that there was the formation of a hexagonal $D0_{19}$ structure phase in Mg-RE alloys, namely β'', with lattice parameters $a=2a_{\alpha\text{-Mg}}=0.64$ nm, $c=c_{\alpha\text{-Mg}}=0.52$ nm and an

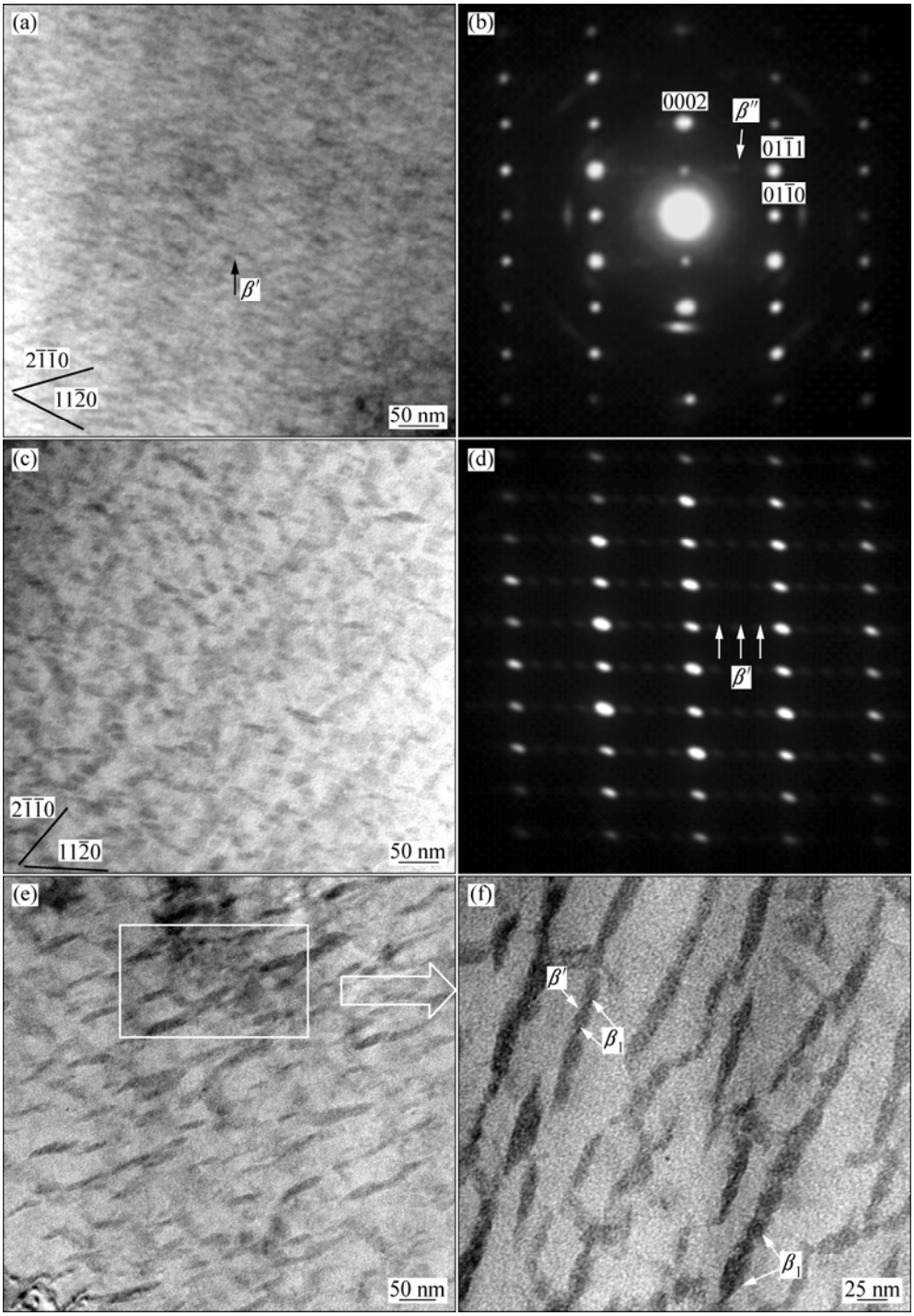

Fig. 2 TEM images recorded from samples aged at 200 °C for different ageing time: (a), (b) Bright-field image and corresponding SAED pattern from half peak-aged (8 h) sample (B//$[2\bar{1}\bar{1}0]_\alpha$); (c), (d) Bright-field images recorded and corresponding SAED pattern from peak-aged (20 h) sample (B//$[2\bar{1}\bar{1}0]_\alpha$); (e), (f) Bright-field images recorded and large amplification image from over-aged (108 h) sample

orientation relationship of $[0001]_{\beta''}$//$[0001]_\alpha$, $(2\bar{1}\bar{1}0)_{\beta''}$// $(2\bar{1}\bar{1}0)_\alpha$. Therefore, the hardening is attributed to the precipitation of β'' and β' phases at the half peak-aged stage in Mg-Gd-Y-Zr alloys. The peak-aged microstructure contains predominantly β' phase (Fig. 2(c)). It is observed that the oval plate-shaped β' precipitates are on $\{11\bar{2}0\}_\alpha$ with three variants. In the peak-aged alloy, the plate-shaped β' phase grows to 30 nm in diameter and is more compared with half peak-aged one. Many researchers [9−11] indicated that the β' phase was the main precipitates for strengthening of Mg-Gd-Y-Zr alloys, and it attributed more to the

hardening than β'' phase. Therefore, the ageing hardening curve reaches peak value when the alloy aged at 200 °C for 20 h, due to the β' phase precipitating completely at this time. The SAED pattern corresponding to Fig. 2(c) is shown in Fig. 2(d), which is in compliance with related report [12]. These small spots at 1/4, 1/2 and 3/4 distance of the $\{1\bar{1}00\}_\alpha$ reflections indicate the formation of β' phase. Figure 2(e) presents TEM image of the microstructure in an over-aged sample (at 200°C for 108 h). The β' phase became coarse with the diameter of 100−150 nm so the β' phase is obviously going to grow with the increase of ageing time. Meanwhile, it is found that some interior sections of the β' phase begin to decompose and a new precipitate phase form from the high amplification image in Fig. 2(f). HE et al [4] reported this new phase named β_1 phase (fcc, a=0.74 nm), and the orientation relationship between β_1 phase and the α-Mg matrix being $[110]_{\beta 1}//[0001]_\alpha$ and $(\bar{1}12)\beta_1//(1\bar{1}00)_\alpha$. It is observed that a β_1 phase is attached to two β' particles shown in Fig. 2(f). Preferential nucleation of β_1 phase in association with the β' particles is suggested to be caused by the following factors [13]: Firstly, the composition difference between β_1 and β' phases is much less than that between β_1 and the α-Mg matrix, so the formation of β_1 phase on β' particles requires much less long-distance diffusion of the RE solutes than the direct nucleation in the matrix; Secondly, the habit plane between the β_1 and β' phases has been measured to be a semi-coherent interface due to the structural similarity. Therefore, the formation of β_1 phase is associated with the β' phase.

3.3 Immersion tests

Figure 3 shows the corrosion rates of Mg-10Gd-4.8Y-0.6Zr alloy aged at 200 °C for 0 h, 1 h, 8 h, 20 h, and 108 h after immersion in 3.5% NaCl solution for 3 d. The mass loss rates of the alloy under five conditions decrease with the increase of the ageing time and the corrosion resistance increases slowly after peak-aged time.

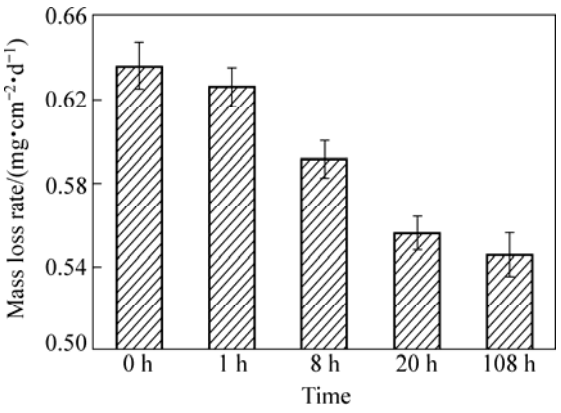

Fig. 3 Corrosion rates of Mg-10Gd-4.8Y-0.6Zr extruded-alloys aged at 200 °C for different time and immersed in 3.5% NaCl solution for 3 d

The morphological characteristics of the corroded surface on the specimens after immersion in 3.5% NaCl solution are shown in Fig. 4. The corrosion spots are distributed on the surface of all corrosion specimens, but there are no deep corrosion pits. The amount of corrosion spots on the specimen surfaces decreases with the increase of ageing time. Evidently, the corrosion of specimen without ageing treatment is the most serious among all the conditions, and the surface becomes darker than other specimens (Fig. 4(a)). For peak-aged (20 h) alloy, the area of corrosion surface without deep corrosion spots begins to enlarge and has the compact white film covered (Fig. 4(d)). The over-aged (108 h) specimen has thicker film on the surface than the peak-aged one (Fig. 4(e)). The surface morphology photographs of the corroded specimens are basically in agreement with the mass loss rates shown in Fig. 3. Meanwhile, it can be found that the precipitate phases become coarse with prolonging the ageing time from the analysis of the ageing precipitation. So the coarse precipitate phase can effectively block the corrosion of the alloy. NORDLIEN et al [14] suggested that the corrosion products of magnesium alloys present three-layered structure, characterized by an outer thick platelet-like porous layer, rich in magnesium hydroxide, a dense thin intermediate MgO region, and hydrated inner MgO-$Mg(OH)_2$ layer. CHANG et al [15] showed that RE element can stabilize these compounds. So the compounds play an important role as a stable compact film on the surface of specimens, resulting in higher corrosion resistance.

3.4 Electrochemical measurement

3.4.1 Open circuit potential

The open circuit potentials of Mg-10Gd-4.8Y-0.6Zr alloy under different ageing conditions are shown in Fig. 5. The evolution of open circuit potential with time is recorded for 20 min. The φ_{OCP} value rises sharply in the initial 5 min of immersion time, and then reaches a stable value after a slight rise due to the stable growth of the protective surface film. It is clearly seen that the stable φ_{OCP} values of specimens under the different ageing conditions have the following rule: they increase with the lengthening of ageing time. The extruded specimen without ageing treatment needs more time to reach the stable value of φ_{OCP}.

3.4.2 Polarization curves

Figure 6 presents the potentiodynamic polarization curves of the specimens under different ageing conditions in 3.5% NaCl solution saturated with $Mg(OH)_2$. The corrosion potential (φ) and corrosion current density (J) are deduced from the potentiodynamic

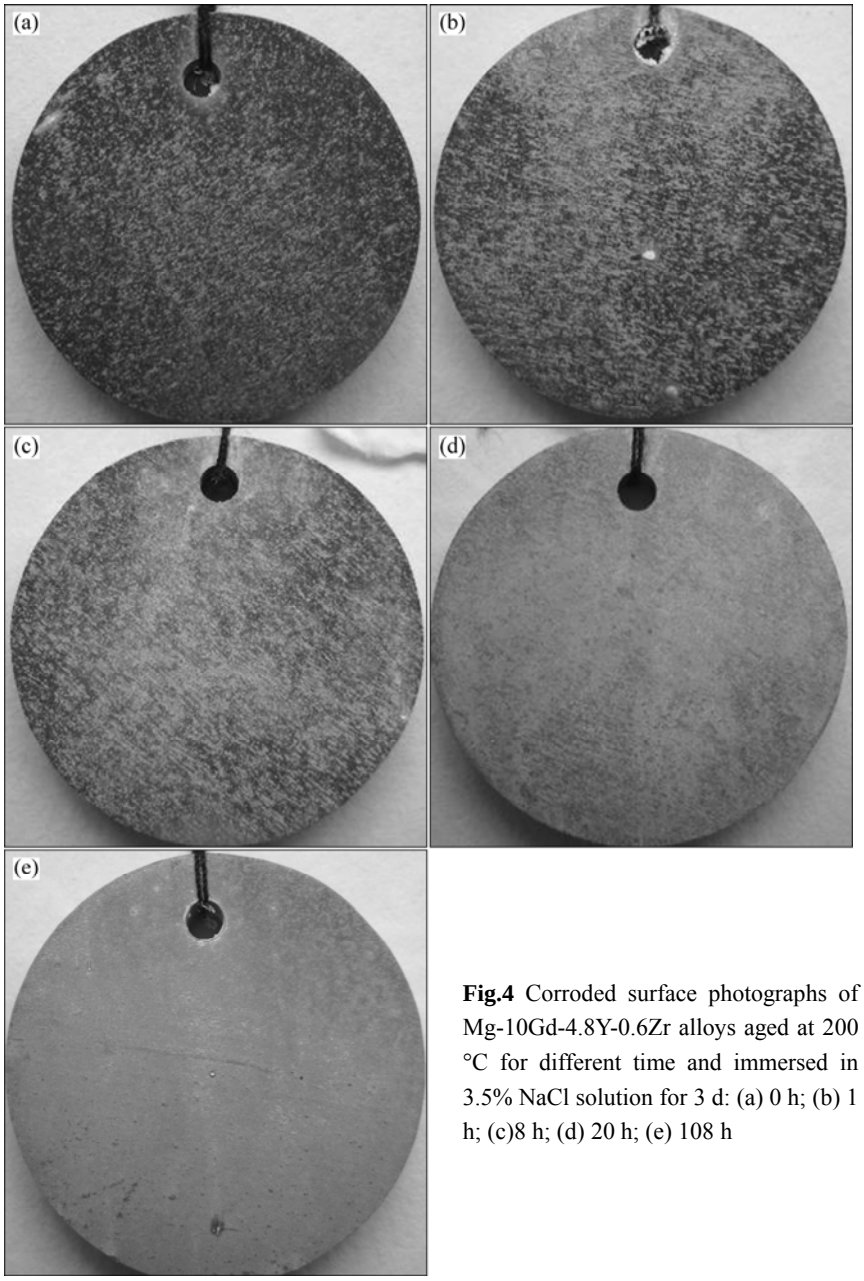

Fig.4 Corroded surface photographs of Mg-10Gd-4.8Y-0.6Zr alloys aged at 200 °C for different time and immersed in 3.5% NaCl solution for 3 d: (a) 0 h; (b) 1 h; (c)8 h; (d) 20 h; (e) 108 h

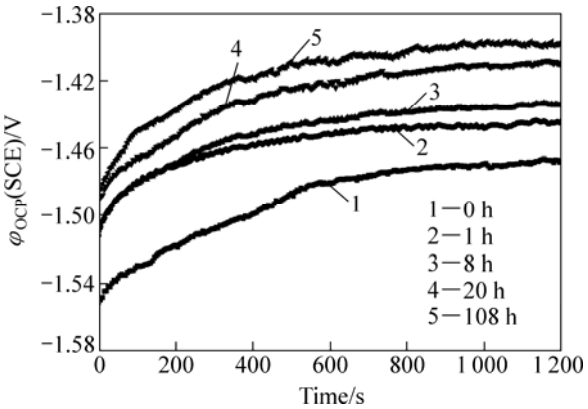

Fig. 5 Variation of corrosion potentials of Mg-10Gd-4.8Y-0.6Zr alloys aged at 200 °C for different time and immersed in 3.5% NaCl solution saturated with $Mg(OH)_2$

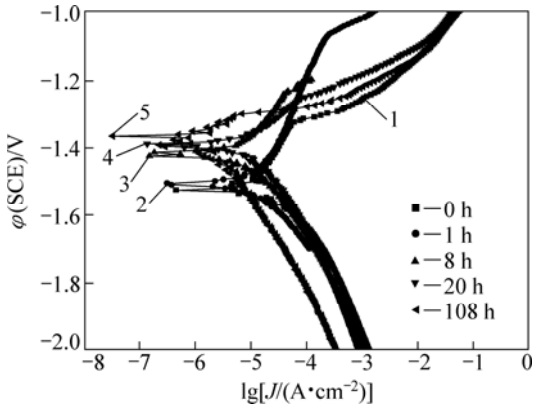

Fig. 6 Polarization curves for Mg-10Gd-4.8Y-0.6Zr alloy aged at 200 °C for different time and immersed in 3.5% NaCl solution saturated with $Mg(OH)_2$

polarization curves. After 20 min of immersion, φ is more and more positive and J is more and more negative with the increase of ageing time. Therefore, judging from the change of corrosion current density, we can find that the corrosion resistance of specimens aged at 200 °C increases with the increase of ageing time.

The cathodic polarization curves are assumed to represent the cathodic hydrogen evolution through water reduction as a reaction, while the anodic ones represent the dissolution of magnesium as a reaction [16]. The cathodic parts of the curves in Fig. 6 suggest that the cathodic polarization current density decreases with the increase of ageing time and the cathodic polarization current of specimen aged for 108 h is much lower than other specimens. This indicates that the cathodic reaction is more and more difficult kinetically on specimens with the increase of ageing time. Meanwhile, the anodic portions of them all exhibit a clear and short current plateau before the breakdown potential (EBD). Then the current density keeps a rapid increasing rate with the increase of potential. The current plateau appears due to the more protective film formed on the surface of the specimens. It can be seen that EBD of extruded alloy without ageing treatment is lower than that of the others.

Compared with polarization curves of Mg-10Gd-4.8Y-0.6Zr alloy under different aged conditions, it is shown that the ageing treatment leads to an increase in the cathodic over-potential with the increase of ageing time, and a decrease in the current density of anodic current plateau. The result of the immersion test (Fig. 3 and Fig. 4) shows the peak-aged and over-aged specimens have the best corrosion resistance, due to the inhibiting effect of higher cathodic over-potential for them gaining the upper hand.

3.4.3 Electrochemical impedance spectroscopy (EIS)

The EIS results of Mg-10Gd-4.8Y-0.6Zr alloy under different ageing conditions are presented in Fig. 7. The Nyquist curve of the extruded specimen without ageing has one capacitive loop in the high frequency and an inductive loop in the low frequency range. The inductive character in the low frequency range indicates that the corrosion product film dissolved faster than formation for the non-aged specimen. Further, compared with the non-aged specimen, the EIS spectra of the extruded specimens with ageing treatment are similar and characterized by one capacitive loop in the high frequency, except for the difference in the diameter of the loops. This means that the corrosion mechanisms of the specimens are the same, but their corrosion rates are different.

Figure 7 shows that the capacitive loops reduce gradually with the increase of ageing time. It suggests that the corrosion rate decreases with the increase of ageing time. Meanwhile, their Nyquist curves present the capacitive character, which indicates that the corrosion product film formed faster than dissolution.

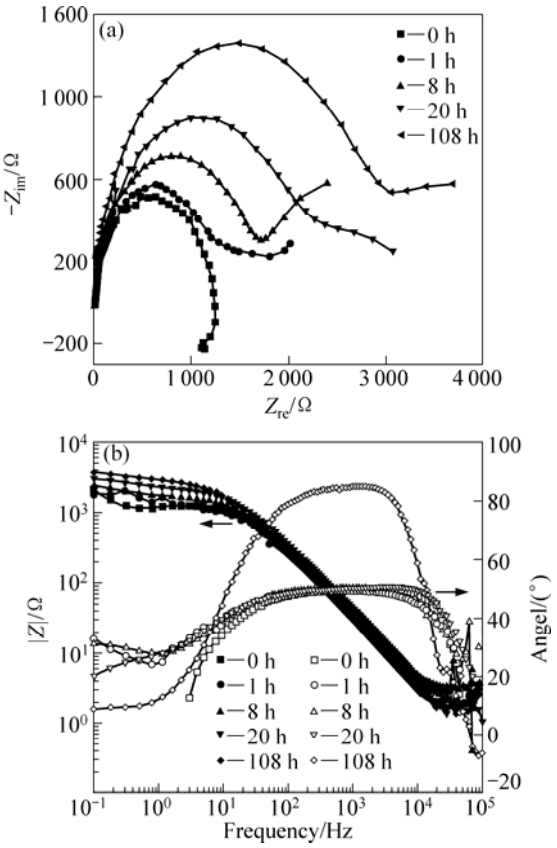

Fig. 7 Nyquist (a) and Bode phase (b) plots of alloy under different ageing conditions after measurement in 3.5% NaCl solution saturated with $Mg(OH)_2$

Therefore, the corrosion product films on the peak-aged and over-aged specimen are clearly seen from Fig. 4.

Based on the characteristics of Nyquist curves, the equivalent circuit models were proposed to analyze the experimental data of EIS for the samples in our study. Figure 8(a) shows the equivalent circuit $[R_s(C_dR_t(R_0L))]$ to analyze the EIS results of the non-aged sample.

For the non-aged sample, the Nyquist plots of the impedance show a loop at the low frequencies due to the formation of pits. This means that an inductor exists in the equivalent circuit. For the samples aged for 1, 8, 20 and 108 h, due to the same characteristics of Nyquist curves, these four ageing conditions have an equivalent circuit $[R_s(C_d(R_c(C_dR_t)))]$ shown in Fig. 9(a). Figures 8(b) and 9(b), (c), (d) show the good correlation between the experimental curves and the curves obtained in a simulation using the corresponding equivalent circuits proposed. The estimated values obtained by Zview software for each electric component are shown in Table 1. It can be seen that the resistance of the corrosion

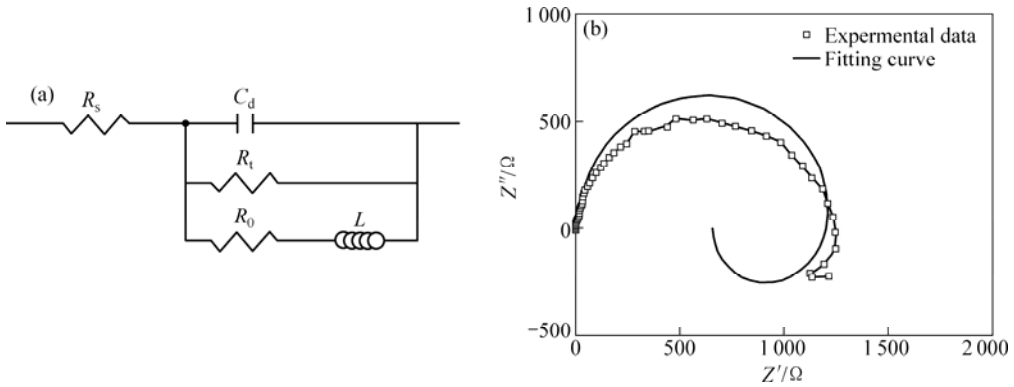

Fig. 8 Equivalent circuit model (a) and fitting EIS data (b) for non-aged sample and corresponding simulated curve

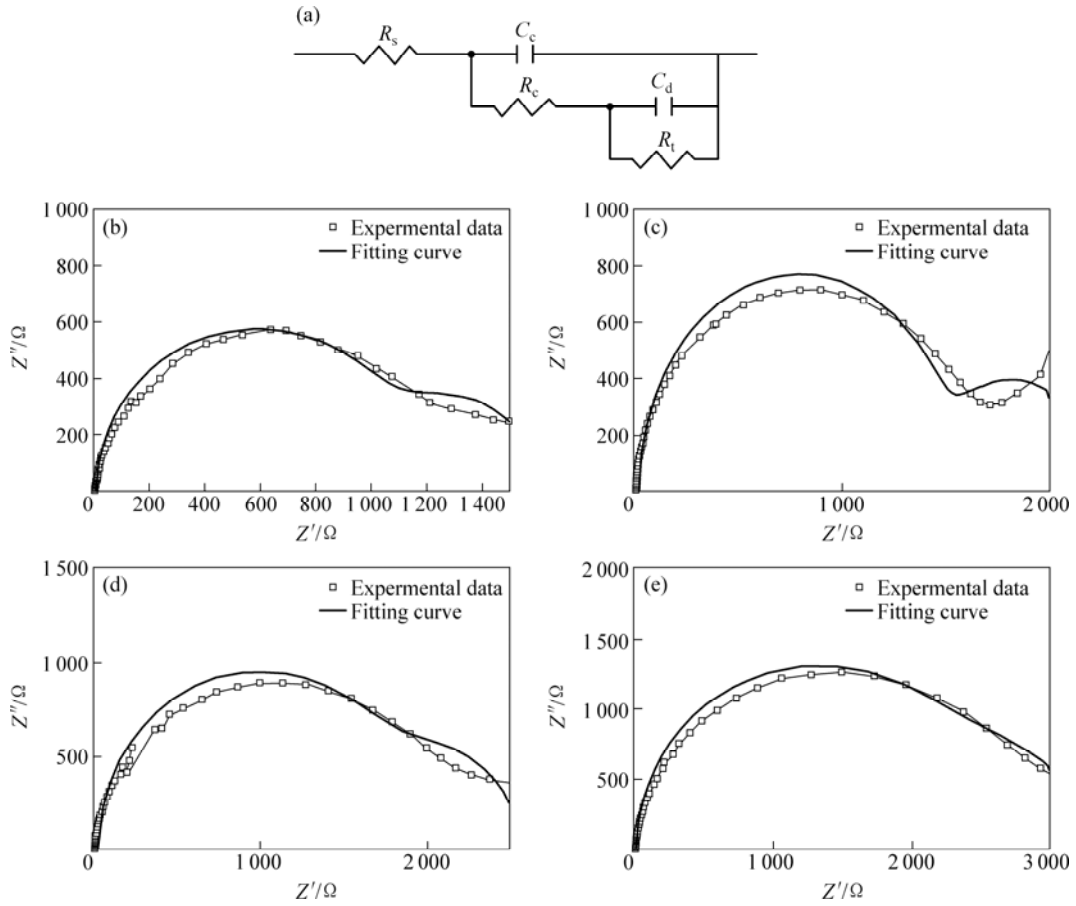

Fig. 9 Equivalent circuit model (a) and EIS data for samples aged for 1 h (b), 8 h (c), 20 h (d), 108 h (e) and corresponding simulated curves

Table 1 Values of circuit elements in equivalent circuit

Ageing time/h	R_s/(Ω·cm^{-2})	C_d/(10^{-4}F·cm^{-2})	R_0/(Ω·cm^{-2})	R_c/(Ω·cm^{-2})	L/μH	C_c/(10^{-6}F·cm^{-2})	R_t/(Ω·cm^{-2})
0	10	1.50	1 350	−	45	−	1 250
1	10	1.30	−	1 150	−	4.2	450
8	23	1.20	−	1 540	−	1.8	650
20	30	1.17	−	1 910	−	1.6	615
108	10	1.10	−	2 600	−	1.2	650

solution is very low. The C_d value decreases with the increase of the ageing time, but R_c value increases due to the increase in denseness of the corrosion product film with the increase in the ageing time. Therefore, the results of EIS are in agreement with the morphologies of the corrosion film.

4 Conclusions

1) The corrosion rate of Mg-10Gd-4.8Y-0.6Zr alloy decreases with the increase of the ageing time from 0 to 108 h. The corrosion resistance of the experimental alloy was found to increase with the increase in the size of the precipitate phases. The coarse phase can act as a compact barrier to decrease the corrosion rate. The denseness of corrosion film increases with the increase in the ageing time.

2) The φ_{OCP} of Mg-10Gd-4.8Y-0.6Zr alloy increases with the increase of the ageing time. The potentiodynamic polarization curves show that the ageing treatment leads to an increase in the cathodic over-potential (inhibiting effect) with the increase of ageing time, and a decrease in the current density of anodic current plateau (accelerating effect) with the increase of ageing time. The equivalent circuit of the non-aged sample is $[R_s(C_dR_t(R_0L))]$ and that of the aged samples is $[R_s(C_d(R_c(C_dR_t)))]$.

References

[1] ANYANWU I A, KAMADO S, KOJIMA Y. Aging characteristics and high temperature tensile properties of Mg-Gd-Y-Zr alloys [J]. Materials Transactions, 2001, 42(7): 1206−1211.

[2] MORDIKE B L. Creep-resistant magnesium alloys [J]. Materials Science and Engineering A, 2002, 324(1−2): 103−112.

[3] WANG Jie, ZHOU Ji-xue, TONG Wen-hui, YANG Yuan-sheng. Effect of purification treatment on properties of Mg-Gd-Y-Zr alloy [J]. Transactions of Nonferrous Metals Society of China, 2010, 20(7): 1235−1239

[4] HE S M, ZENG X Q, PENG L M, GAO X, NIE J F, DING W J. Microstructure and strengthening mechanism of high strength Mg-10Gd-2Y-0.5Zr alloy [J]. Journal of Alloys and Compounds, 2007, 427(1−2): 316−323.

[5] GAO Lei, CHEN Rong-shi, HAN En-hou. Fracture behavior of high strength Mg-Gd-Y-Zr magnesium alloy [J]. Transactions of Nonferrous Metals Society of China, 2010, 20(7): 1217−1221.

[6] XIAO Y, ZHANG X M, CHEN B X, DENG Z Z. Mechanical properties of Mg-9Gd-4Y- 0.6Zr alloy [J]. Transactions of Nonferrous Metals Society of China, 2006, 16(3): 1669−1672.

[7] KAWABATA T, FUKUDA Y, MATSUDA K, KAMADO S, KOJIMA Y, IKENO S. HRTEM observation of age hardening precipitates in Mg-8.3%Gd-3.7%Y-0.76%Zr alloy [J]. Materials Transactions, 2007, 48(5): 954−959.

[8] HONMA T, OHKUBO T, HONO K, KAMADO S. Chemistry of nanoscale precipitates in Mg-2.1Gd-0.6Y-0.2Zr (at.%) alloy investigated by the atom probe technique [J]. Materials Science and Engineering A, 2005, 395(1−2): 301−306.

[9] PENG Q M, WU Y M, FANG D Q, MENG J, WANG L M. Microstructures and properties of Mg-7Gd alloy containing Y [J]. Journal of Alloys and Compounds, 2007, 430(1−2): 252−256.

[10] LIU X B, CHEN R S, HAN E H. Effects of ageing treatment on microstructures and properties of Mg-Gd-Y-Zr alloys with and without Zn additions [J]. Journal of Alloys and Compounds, 2008, 465(1−2): 232−238.

[11] LIU Ke, ZHANG Jing-huai, TANG Ding-xiang, ROKHLIN L L, ELKIN F M, MENG Jian. Precipitates formed in a Mg-7Y-4Gd-0.5Zn-0.4Zr alloy during isothermal ageing at 250°C [J]. Materials Chemistry and Physics, 2009, 117(1): 107−112.

[12] HONMA T, OHKUBO T, KAMADO S, HONO K. Effect of Zn addition on the age-hardening of Mg-2.0Gd-1.2Y-0.2Zr alloys [J]. Acta Materialia, 2007, 55(12): 4137−4150.

[13] GAO X, HE S M, ZENG X Q, PENG L M, DING W J, NIE J F. Microstructure evolution in a Mg-15Gd-0.5Zr (wt.%) alloy during isothermal aging at 250 °C [J]. Materials Science and Engineering A, 2006, 431(1−2): 322−327.

[14] NORDLIEN J H, NISANCIOGLU K, ONO S, MASUKO N. A TEM investigation of naturally formed oxide films of pure magnesium [J]. Corrosion Science, 1997, 39(8): 1397−1414.

[15] CHANG Jian-wei, GUO Xing-wu, FU Peng-huai, PENG Li-ming, DING Wen-jiang. Effect of heat treatment on corrosion and electrochemical behaviour of Mg-3Nd-0.2Zn-0.4Zr (wt.%) alloy [J]. Electrochimica Acta, 2007, 52 (9): 3160−3167.

[16] CHANG Jian-wei, GUO Xing-wu, FU Peng-huai, PENG Li-ming, DING Wen-jiang. Investigation of the corrosion for Mg-*x*Gd-3Y-0.4Zr (*x*=6, 8, 10, 12 wt.%) alloys in a peak-aged condition [J]. Corrosion Science, 2008, 50 (1): 166−177.

时效时间对挤压 Mg-10Gd-4.8Y-0.6Zr 合金腐蚀性能的影响

李慧中[1,2,3]，刘洪挺[1]，郭菲菲[1]，王海军[1]，梁霄鹏[1,2]，刘楚明[1]

1. 中南大学 材料科学与工程学院，长沙 410083；
2. 中南大学 粉末冶金国家重点实验室，长沙 410083；
3. 中南大学 有色金属材料科学与工程教育部重点实验室，长沙 410083

摘 要：采用浸泡实验和电化学分析，探讨时效过程中挤压 Mg-10Gd-4.8Y-0.6Zr 合金的腐蚀行为。结果表明：合金的腐蚀速率随着时效时间的延长而逐渐减小；合金抗腐蚀性能随着时效析出相的长大、粗化而逐渐提高；开路电位随着时效时间的延长而逐渐变正。由极化曲线可知，在时效处理中，阴极电位和阳极电流的平稳期发生改变，阴极电位随着时效时间的延长而增加(抑制效应)，而阳极电流的平稳期随着时效时间的延长而降低(催化效应)。

关键词：Mg-10Gd-4.8Y-0.6Zr 合金；腐蚀行为；时效时间

(Edited by YANG Hua)